KeAi

CHINESE ROOTS
GLOBAL IMPACT

Contents lists available at ScienceDirect

Petroleum Science

journal homepage: www.keaipublishing.com/en/journals/petroleum-science



Original Paper

Sandstone breaking performances and mechanisms of swirling abrasive waterjet during radial jet drilling process



Huan Li, Jing-Bin Li *, Chen-Rui Guo, Hao Wang, Rui Li, Zhong-Wei Huang

State Key Laboratory of Petroleum Resources and Prospecting, China University of Petroleum (Beijing), Beijing, 102249, China

ARTICLE INFO

Article history: Received 15 January 2024 Received in revised form 30 May 2024 Accepted 31 May 2024 Available online 1 June 2024

Edited by Jia-Jia Fei

Keywords:
Development of unconventional oil and gas
Abrasive waterjet
Radial jet drilling
Sandstone breakage

ABSTRACT

Radial jet drilling (RJD) is one of the emerging hydrocarbon drilling technologies. And, the swirling abrasive waterjet (SAWJ) is expected to drill larger diameter laterals during RJD. Here, the performances and mechanisms of SAWJ breaking sandstone were studied by laboratory experiments. Results showed that the SAWJ could drill a smooth (surface roughness was 0.043 mm) & large (diameter was in 52.0 -73.0 mm) circular hole on sandstone. The hole depth/volume increased as the jetting pressure, abrasive mass concentration and exposure time increased. Conversely, they decreased as the standoff distance increased. The optimal parameter combination under our experimental conditions was 30 MPa, 0 mm, 12% and 1 min. The SAWJ sandstone breaking mechanism were the erosion of cements, the integrally peeled off and broken of crystal grain. Failure mode of sandstone was mainly the tensile fracture. The key findings will provide guidance for the application of SAWJ in RJD technology.

© 2024 The Authors. Publishing services by Elsevier B.V. on behalf of KeAi Communications Co. Ltd. This is an open access article under the CC BY-NC-ND license (http://creativecommons.org/licenses/by-nc-nd/4.0/).

1. Introduction

As the main energy source in the world, conventional fossil fuels have a significant impact on various aspects of societal advancement. With the increased demand of oil and gas, it's necessary to develop the unconventional oil and gas. Shale gas (He et al., 2023), shale oil (Xu et al., 2022), tight oil (Jia et al., 2012), tight sandstone gas (Ma et al., 2016) are the vital part of unconventional oil and gas, and they are extreme hard to be developed with traditional technology. Fracturing technique makes it possible to realize the commercial exploitation of unconventional oil and gas. Unfortunately, conventional fracturing technique uses water as fracturing fluid, which consumes vast quantities of water resources and is difficult to carry out in water shortage area (Wen et al., 2023; Yang et al., 2023). Based on this, lots of new fracturing techniques (LN₂ fracturing, SC-CO₂ fracturing and so on) are put forward and experimentally investigated (Kalam et al., 2021; Mojid et al., 2021). Different from traditional hydraulic fracturing method, SC-CO₂ fracturing and LN₂ fracturing are water-free and green fracturing techniques for unconventional oil and gas development. Furthermore, they have the ability to generate more intricate fracture networks than conventional hydraulic fracturing under same conditions. However, the proppant carrying abilities of the SC-CO₂ and LN₂ are poor because the density and viscosity of them are low (Wen et al., 2023). The output of unconventional oil and gas reservoirs increases with an increase in the proppant pumped in (LaFollette et al., 2014; Pankaj et al., 2018). Thus, disadvantages of poor proppant carrying ability limits stimulation performance of SC-CO₂ fracturing and LN₂ fracturing. Therefore, it's essential to develop an innovative stimulation treatment for cost-effective and environmentally friendly exploitation of unconventional oil and gas.

RJD technology is an innovative oil and gas drilling & development method in the 21st century (Kamel, 2017; Li et al., 2021; Salimzadeh et al., 2019). Copious case studies across the globe have substantiated that RJD is a practical substitute for customary stimulation methods (Asgharzadeh et al., 2017; Ashena et al., 2020; Nagar et al., 2020). RJD usually utilizes the energy produced by high velocity water/abrasive slurry to drill radial holes from main wellbore. It can create a well structure with the characteristics of multi layers and multi laterals in both conventional and unconventional reservoirs. The diameter of the RJD-drilled holes is up to 50 mm and lengths up to 100 m (Huang et al., 2018, 2020; Kamel, 2017). Thus, it can significantly extend past the damaged area of the wellbore and provide efficient flow channels for oil and gas. Furthermore, the combination of fracturing technology and RJD technology, which is

E-mail address: lijb@cup.edu.cn (J.-B. Li).

^{*} Corresponding author.

called the radial-borehole fracturing, can three-dimensional fracturing the reservoirs and is regarded as an innovative and cost-effective fracturing technique (Guo et al., 2022; Salimzadeh et al., 2020; Wang et al., 2023). The current studies about RJD technique are mainly RJD exploitation method & productivity & fracturing (Gong et al., 2016; Li et al., 2020; Yang et al., 2019). It needs to be emphasized that successful drilling of radial branches is a prerequisite for these techniques that based on RJD. The key difference between traditional drilling technology and RJD technology is the rock-breaking strategy. The traditional drilling technology utilizes mechanical energy of a PDC bit (Fig. 1) to break rock (Xiong et al., 2022), while the RJD technology utilizes hydraulic energy of a jet nozzle (Fig. 2) to break rock (Li et al., 2020). Therefore, the jet nozzle holds a significant position in RJD and it's one of the key factors that determine the success of a RJD operation.

Jet nozzles applied for RJD technology are conical nozzle, swirling impeller nozzle, straight swirling mixed nozzle, etc. Jet rock breakage characteristics of different nozzles using different jet medium on different target rock are listed in Table 1 (Du et al., 2022; Fu et al., 2021; Hong et al., 2021; Li et al., 2022; Li et al., 2020; Yang et al., 2019, 2022). It's obviously that SAWJ boasts the finest rock drilling capability among them. Not only soft coal rock, but also hard granite can be effectively drilled by SAWJ. Diameter of the SAWJ-drilled hole on coal is about 2.9 times of the conical abrasive liquid nitrogen jet drilled-hole and 2.0 times of the hole drilled by conical nozzle using abrasive nitrogen gas slurry. Besides, the SAWJ can create a regular hole with a 56.3 mm diameter on hard granite. Although the SAWI-drilled hole diameter on granite is only 59.9% of the SAWI-drilled hole diameter on coal, it still completely satisfied the requirement of RJD technology. The SAWI have be proven to be a feasible method to drill large diameter holes within common rocks, such as shale, coal rock, limestone, sandstone and granite (Zhou et al., 2023). The study of SAWJ was still in its early stages. Chen et al. (2021) analyzed the characteristics and evolution of swirling water jet flow field through numerical simulation. The results indicated that the swirling water jet has the characteristic of strong diffusivity, which means it has a large impact area and a short effective impact distance. Ma et al. (2021) carried out limestone breaking experiments with SAWJ, the findings indicated that the diameter of holes tended to increase as the standoff distance and abrasive mass concentration increased. Yang



Fig. 1. PDC bite for traditional drilling.

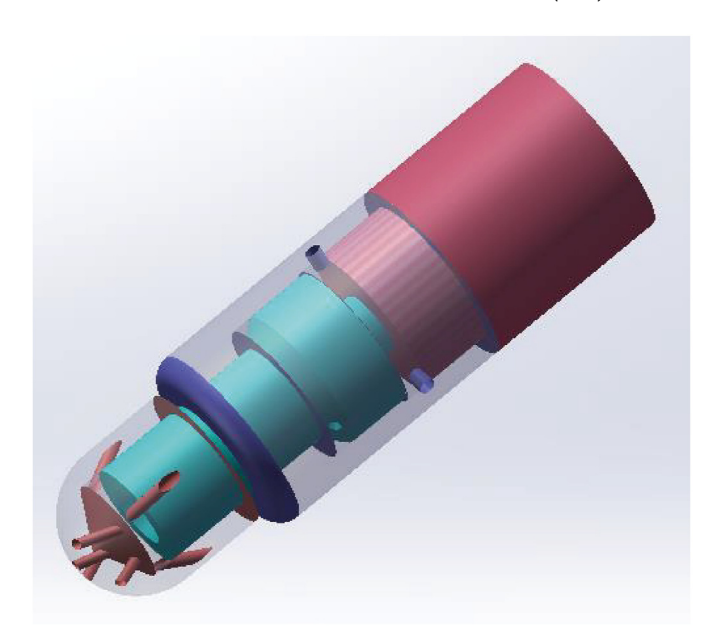


Fig. 2. Jet nozzle for RJD.

et al. (2022) conducted coal breaking experiments with SAWJ, the results showed that the hole diameter was 71 mm when jetting at a distance of 50 mm perpendicular to the bedding plane. Besides, the hole diameter was 94 mm when jetting at the same distance parallel to the bedding plane. They think the stratification cracking along the weak planes was the most important coal-breaking mechanism. Li et al. (2022) carried out granite breaking experiments with SAWJ, and they further investigated the practicability of SAWJ drilling in hard rocks. Currently, studies about SAWJ are concentrated on the rock drilling feasibility. Although the effect of parameters during SAWJ drilling is of great practical significance, literature investigate indicates that there are few studies related to it.

In this study, the effect of process parameters (such as jetting pressure, exposure time, etc.) on the SAWJ sandstone drilling performances were investigated with laboratory experiments. Diameter, depth and volume of the hole were used for evaluating the SAWJ sandstone breaking performance under different parameter combinations. Besides, the optimal parameter combination was revealed under certain conditions. Further, scanning electron microscopy (SEM) was assisted in analyzing the microstructure of the hole. Finally, the hole morphology evolution and the rock breakage mechanisms were discussed. The findings of this study provide a theoretical foundation for the operation parameter selection during sandstone radial SAWJ drilling.

2. Experimental methods

2.1. Experimental device

The SAWJ sandstone breaking experiments were conducted with the high-pressure abrasive waterjet rock breaking laboratory system. Work principle of the laboratory system is summarized as Fig. 3. First, abrasive slurry is obtained from the mixing tank. Then, a centrifugal pump transports the abrasive slurry to the plunger pump. It's worth noting that the plunger pump is a kind of fracturing pump, and the abrasive slurry is directly pressurized by it. However, the pump of commercial abrasive waterjet cutting system can only pressurize the pure water. Finally, the plunger pump pressurizes the abrasive slurry, and a SAWJ is formed as the slurry

Table 1Jet nozzles for RJD technology and their rock breaking performance.

Nozzle type	Jet medium	Specimen	Hole characteristics	Max hole diameter
Direct-rotating mixed-jet	Water	Sandstone	A regular hole with a small central boss at the hole bottom.	21.6 mm (Fu et al., 2021)
Conical jet nozzle	Abrasive nitrogen-gas	Coal	A smooth and regular circular hole.	47.0 mm (Hong et al., 2021)
Straight-swirling mixed jet nozzle	Water	Sandstone	A large diameter hole with a low bottom bulge	19.0 mm (Du et al., 2022)
Conical jet nozzle	Abrasive liquid nitrogen	Coal	A spindle shaped hole	32.0 mm (Yang et al., 2019)
Swirling impeller nozzle	Abrasive water slurry	Coal	A large diameter hole with a low bottom bulge	94.0 mm (Yang et al., 2022)
Swirling impeller nozzle	Abrasive water slurry	Granite	A large diameter hole with a high bottom bulge	56.3 mm (Li et al., 2022)

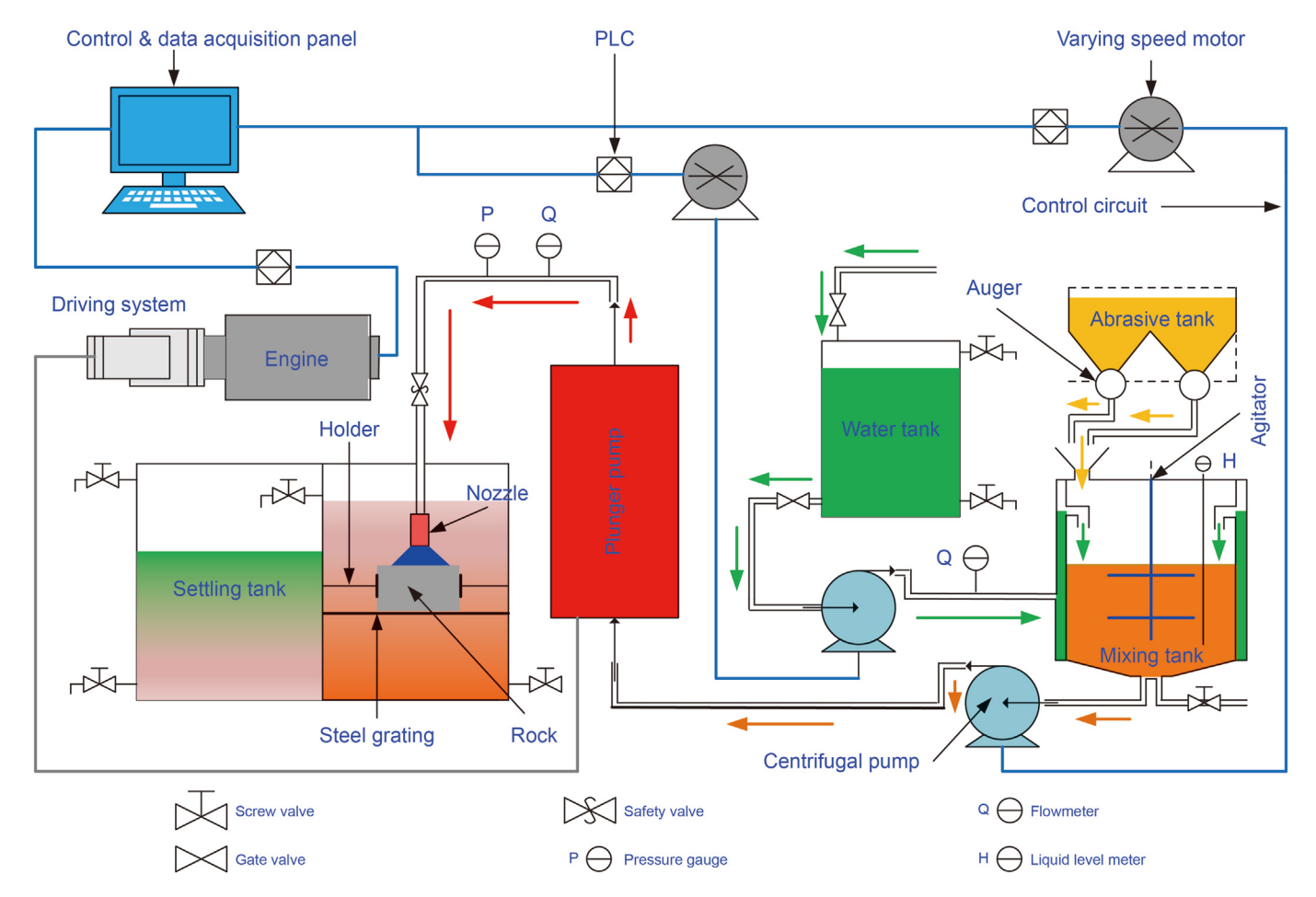


Fig. 3. Schematic of the high-pressure abrasive waterjet rock breaking laboratory system (Green arrows illustrate the trajectory of water, yellow arrows illustrate the trajectory of abrasive, orange arrows illustrate the trajectory of abrasive slurry, red arrows illustrate the trajectory of high-pressure abrasive slurry.

passes through the swirling impeller nozzle. Utmost experimental condition of the laboratory system is jetting pressure 70 MPa, standoff distance 300 mm, sample dimension $400 \times 400 \times 400$ mm, abrasive mass concentration 30%. Physical map of the high-pressure abrasive waterjet rock breaking laboratory system is shown in Fig. 4. Detailed description of the laboratory system can be found in our previous works (Yang et al., 2022; Li et al., 2023).

2.2. Materials

2.2.1. Abrasive material

Abrasive material is one of the crucial parts of a SAWJ rock breakage process. In this study, we choose 46 mesh garnet as abrasive for its good cost performance (Li et al., 2023). Table 2 presents the properties of the used abrasive material in this research.

2.2.2. Rock specimens

Target rock material is sandstone, which is came from Sichuan, China. The size of all sandstone specimens is $150 \times 150 \times 150$ mm. The geo-mechanical properties are shown in Table 3. The sandstone's UCS is 96.10 MPa. And according to the ISRM classification (Barton, 1978), it belongs to strong rock (grades R4, 50 MPa < UCS <100 MPa). Mineral composition of the sandstone is listed in Table 4. It's clear that the quartz (36.4%) and dolomite (46.6%) are the main components of the sandstone.

2.2.3. Swirling impeller nozzle

Swirling impeller nozzle is composed of two parts that are impeller and shell, respectively. As shown in Fig. 5(a), the impeller has three blades which twist into a triple helix structure. The torsion angle and thickness of the blades is 360° and 3 mm, respectively. Besides, the diameter and length of the impeller is 18 and 50 mm, respectively. And, the cross-sectional area of the impeller is







Fig. 4. Physical map of the high-pressure abrasive wateriet rock breaking laboratory system.

Table 2Basic parameters of garnet abrasive.

Ture density, g/cm ³	Mohs hardness	Shape factor	Median diameter, mm	Price, RMB/kg
3.80	8.0	0.764	0.416	2.5

Table 3 Sandstone sample's geo-mechanical properties at 25 $^{\circ}$ C.

Properties	Unit	Value
Density ρ	g/cm ³	2.51
Uniaxial compressive strength UCS	MPa	96.10
Tensile strength T	MPa	9.10
Elastic modulus E	MPa	28.75
Poisson's ratio ν	_	0.22
Porosity Φ	%	7.77
Permeability κ	mD	0.043

Table 4 Mineral composition of sandstone.

Quartz, %	K-feldspar, %	Calcite, %	Dolomite, %	Clay, %
36.4	0.4	13.4	46.6	3.2

83.07 mm³. Three helical flow channel is produced by the combination of impeller and shell. The abrasive slurry will swirl when it flows through the helical flow channel and that makes the SAWJ have a large impact area. As illustrated in Fig. 5(b), the inlet and outlet diameter of the swirling impeller nozzle are 18 and 5 mm respectively. The material of the nozzle is high-strength & highly wear-resistant metal, but its actual life still does not exceed 5 h under our experimental conditions because of the particle abrasion.

2.3. Experimental design

SAWI sandstone breaking experiments are carried out in an

underwater environment at a depth of 550 mm with different operation parameter combinations. Single variable method is adopted to investigate the rock breaking performance with different variables. The experimental schemes can be found in Table 5. The specific experimental operation procedure is detailly described in our previous works (Yang et al., 2022; Li et al., 2023).

3. Results and analysis

3.1. Rock breaking characteristics

Jet-rock breaking characteristics refers to the hole shape, diameter, depth and volume. And, it is usually utilized to evaluate the jet rock breakage ability and RJD feasibility. Morphology of a typical SWAJ-drilled hole on sandstone is shown in Fig. 6. It's obviously that the SAWJ drilled a large circular hole on sandstone. However, the SAWJ couldn't efficiently erode the rock mass located on the jet axis. The hole profile is represented through the longitudinal section of the hole. As shown in Fig. 7, the profile exhibits a W shape. Besides, the hole' wall is smooth and its surface roughness is 0.043 mm which is only 22.6% of the hole on the granite at the same condition (Li et al., 2022). The smoother the SAWJ-drilled hole wall, the smaller the pressure loss in the annulus between the hole and hose (Wang et al., 2016). Further, the smooth hole wall can reduce the friction force on the jet nozzle assembly. These will be beneficial for the RJD operation and the extending of the radial laterals (Li et al., 2015).

The hole diameter, depth and volume on sandstone and granite at the same experimental condition are shown in Figs. 8, 9 and 10

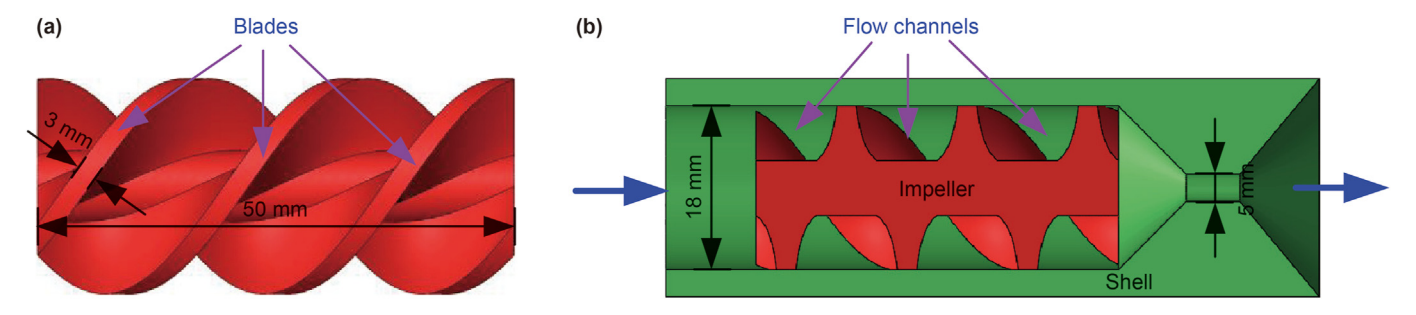


Fig. 5. The swirling impeller nozzle is composed of an impeller (a) and a shell (b).

Table 5 Experimental scenarios.

Jetting pressure, MPa	Standoff distance, mm	Abrasive mass concentration, %	Exposure time, min
10/15/20/25/30	10	10	1
20	0/10/20/30/40/50/60	10	1
20	10	10	1
20	10	4/6/8/10/12	1
20	10	10	1/2/3/4/5

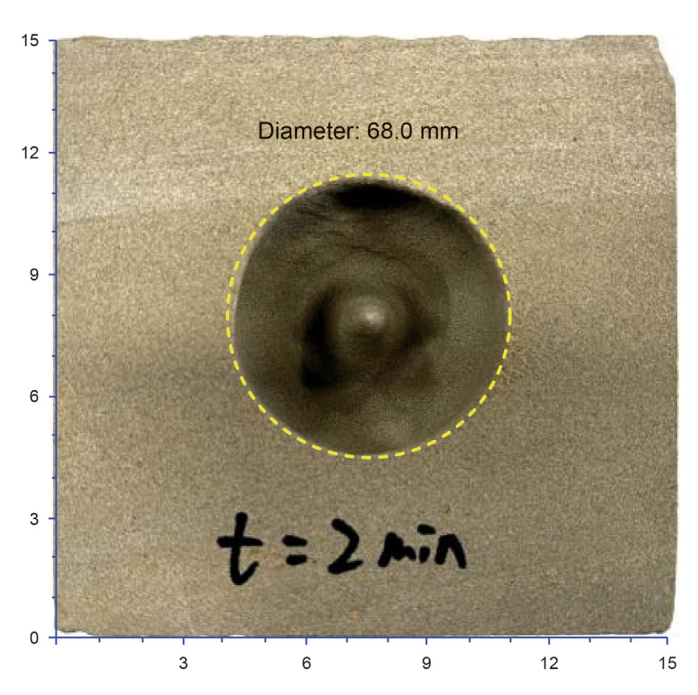


Fig. 6. SAWJ-drilled hole morphology when the standoff distance, jetting pressure, abrasive mass concentration and exposure time are 10 mm, 20 MPa, 10% and 2 min, respectively.

respectively. Specifically, the experiment scenario was the nozzle outlet diameter, jetting pressure, standoff distance, particle size, abrasive mass concentration and exposure time which are 5 mm, 25 MPa, 10 mm, 46 mesh, 10% and 1 min, respectively. It can be found in Fig. 8 that the hole diameter on sandstone and granite are both greater than 30 mm (the critical diameter of RJD operation), which indicates that the SAWJ is one of the possible radial branches drilling methods. Further, the diameter of the hole on sandstone is 1.31 times the diameter on granite. This is because the mechanical strength of granite is greater than sandstone. It can be found in Fig. 9 that the depth of the hole on sandstone is 1.67 times the depth on granite, and that means the effective standoff distance of a SAWJ on sandstone will be greater than that on granite. It can be

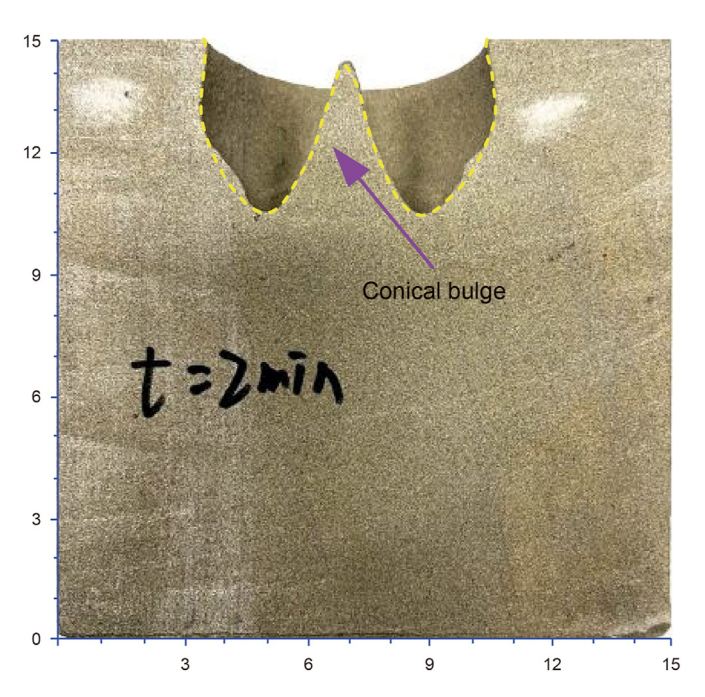


Fig. 7. Longitudinal section of the SAWJ-drilled hole when the standoff distance, jetting pressure, abrasive mass concentration and exposure time are 10 mm, 20 MPa, 10% and 2 min, respectively.

found in Fig. 10 that the volume of the hole on sandstone is 3.83 times the volume on granite, and that means the SAWJ has a better rock breakage efficiency on sandstone rather than that on granite. The previous comparisons have revealed that the SAWJ is more suitable for drilling radial laterals in sandstone formation.

3.2. Effect of jetting pressure

Jetting pressure is the pressure drop when the jetting medium flows through the nozzle. And, it is provided by the pump of the abrasive waterjet machining system. Diameter, depth and volume of the hole on sandstone with various jetting pressures (10–30 MPa) are illustrated in Figs. 11, 12 and 13, correspondingly. It

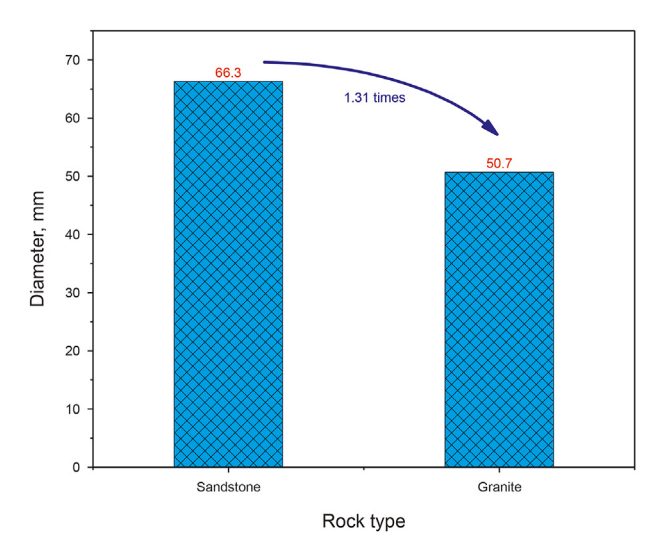


Fig. 8. SAWJ-drilled hole diameter.

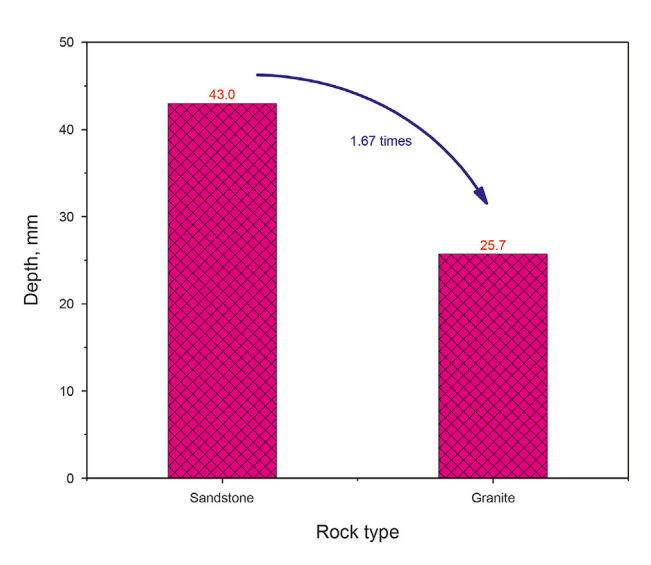


Fig. 9. SAWJ- drilled hole depth.

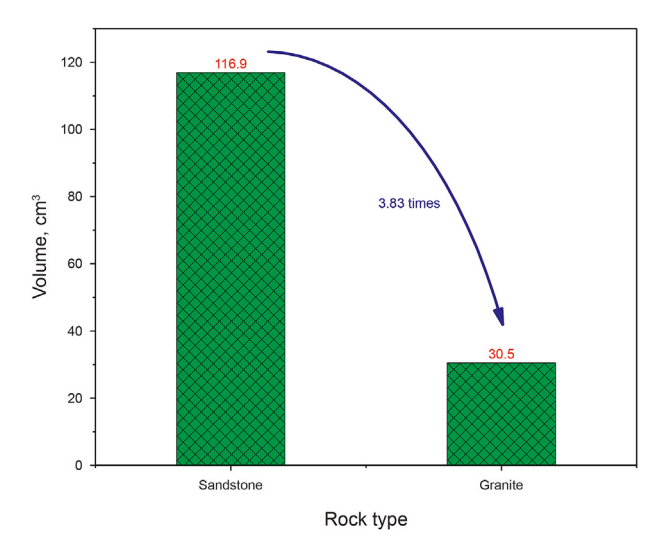


Fig. 10. SAWJ- drilled hole volume.

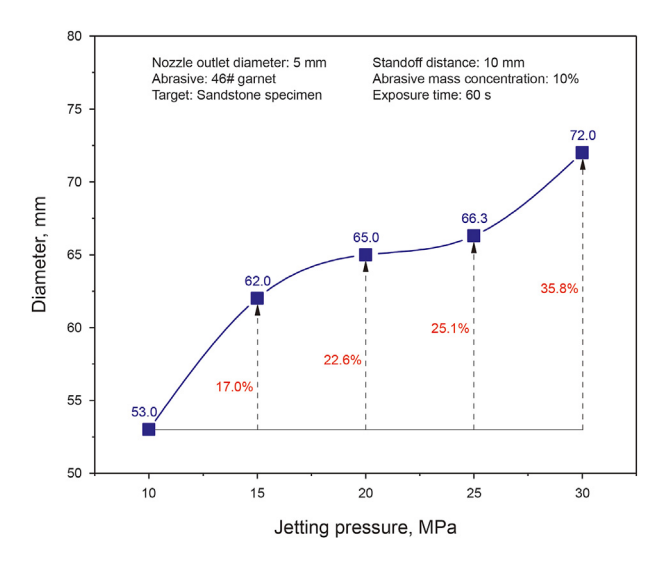


Fig. 11. Hole diameter with jetting pressure.

can be found in Fig. 11 that the hole diameters are in 53.0—72.0 mm and they are all far greater than 30 mm (the critical hole diameter of a successful RJD operation). Besides, the diameter of the hole enlarges as the jetting pressure increases. The hole diameter increases by 35.8% as the jetting pressure increases from 10 to 30 MPa. It can be found in Fig. 12 that the depth of the hole increases as the jetting pressure increases when the jetting pressure ranges from 10 to 25 MPa, but the depth of the hole remains basically unchanged when the jetting pressure ranges from 25 to 30 MPa. The hole depth increases by 42.9% and 44.9% as the jetting pressure is raised from 10 to 25 and 30 MPa, respectively. It can be found in Fig. 13 that the hole volume increases as the jetting pressure increases and it increases by 241.6% as the jetting pressure is raised from 10 to 30 MPa.

The experimental results with various jetting pressures indicated that the rock breaking performance gets better as the jetting pressure increases. Jet-rock breaking is a process of an energy conversion between the jet kinetic energy and the rock surface energy. The effective SAWJ kinetic energy can be regard as the abrasive particles kinetic energy and it can be written as Eq. (1) (Oh and Cho, 2016). Further, based on the nozzle pressure drop formula

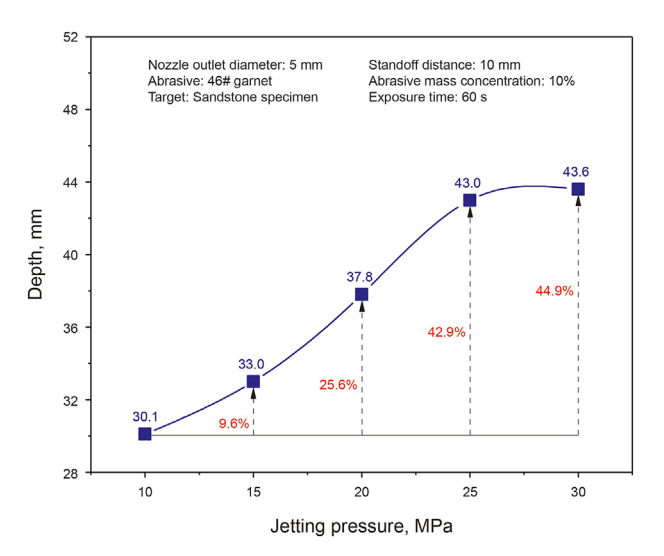


Fig. 12. Hole depth with jetting pressure.

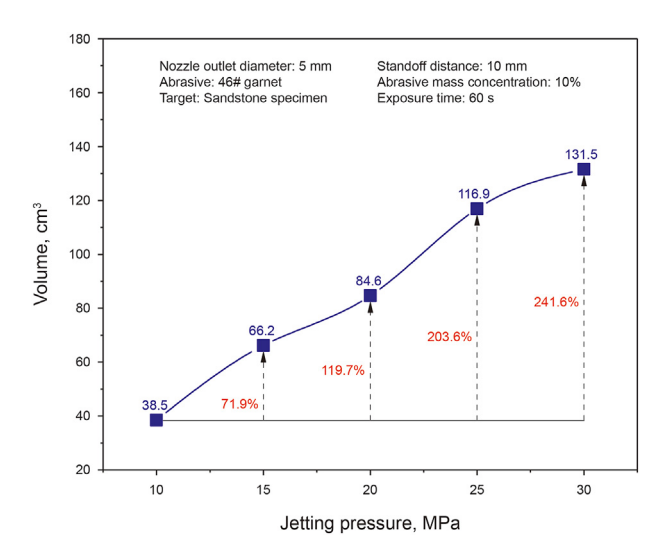


Fig. 13. Hole volumer with jetting pressure.

proposed by Li et al. (2020), the jet velocity can be denoted as Eq. (2). Substituting Eq. (2) into Eq. (1), the effective jet kinetic energy can be written as Eq. (3). It's obviously that the effective kinetic energy is correlated linearly with the jetting pressure. Thus, the larger the jetting pressure, the larger the effective kinetic energy and the better the rock breaking performance. It should be emphasized that the jetting pressure is limited by the equipment such as the pumps and pipes. As analyzed above, the optimal jetting pressure is 30 MPa under our experimental conditions.

$$E_{\text{effective}} = E_{\text{abrasive}} = \frac{1}{2} m_{\text{a}} v^2 t \tag{1}$$

$$v = \sqrt{\frac{PC^2}{\rho}} \tag{2}$$

$$E_{\text{effective}} = \frac{m_a P C^2}{2\rho} t = k_1 P \left(k_1 = \frac{m_a C^2 t}{2\rho} = \text{constant} \right)$$
 (3)

where $E_{\text{effective}}$ represents the effective jet kinetic energy, E_{abrasive}

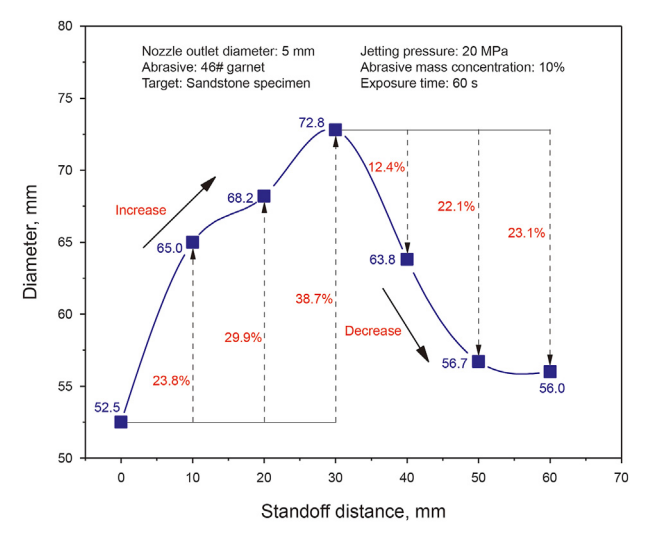


Fig. 14. Hole diameter with standoff distance.

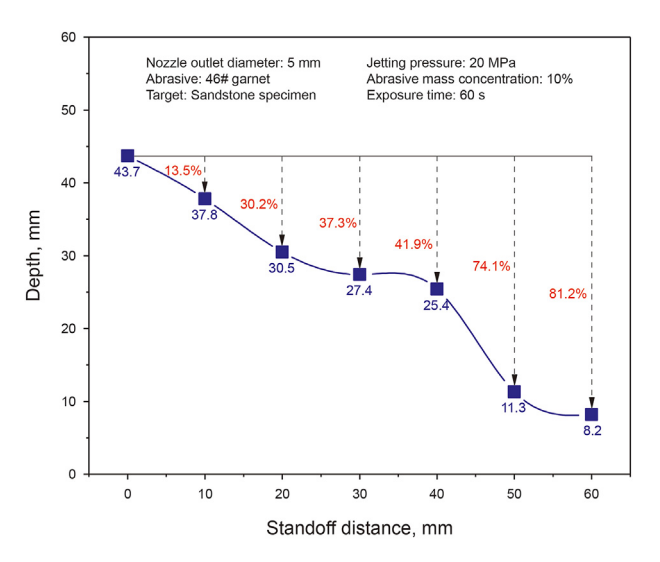


Fig. 15. Hole depth with standoff distance.

represents the abrasive kinetic energy, $m_{\rm a}$ represents the abrasive particle flow rate, t represents the jet exposure time, P represents the jetting pressure, C represents the nozzle flow coefficient, ρ represents the jet medium density.

3.3. Effect of standoff distance

Standoff distance can be controlled with great precision during laboratory experiments. However, it's hard to control exactly how long the standoff distance is in a RJD field application because of the uncertainty pipe assembly length (Li et al., 2020), Figs. 14, 15 and 16 illusrate the diameter, depth and volume of the hole with various standoff distances (0-60 mm) correspondingly. It can be found in Fig. 14 that all the hole diameters are greater than 30 mm which is the critical hole diameter of RJD operation. Besides, the diameter of the hole first increase and then decrease as the standoff distance increases, and reaching the maximum value when the standoff distance is 30 mm. The hole diameter increases by 38.7% as the standoff distance expands from 0 to 30 mm. It can be found in Fig. 15 that the hole depth decreases as the standoff distance increases. The depth of the hole decreases by 37.3% and 81.2% as the standoff distance is raised from 0 to 30 and 60 mm, respectively. It can be found in Fig. 16 that the volume of the hole also decreases as

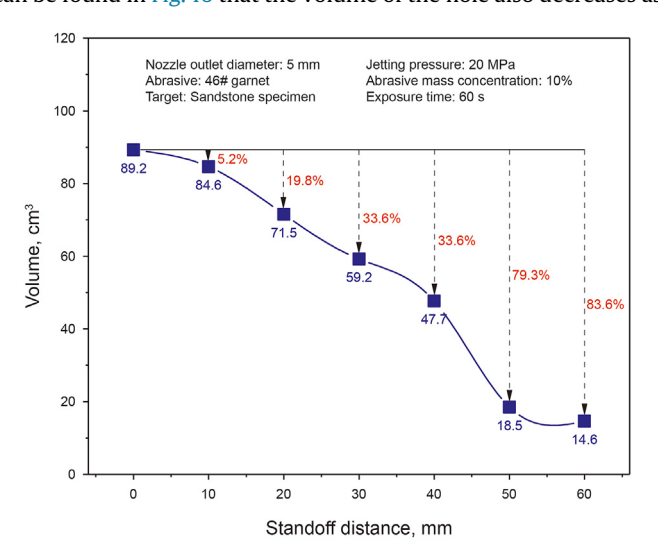


Fig. 16. Hole volume with standoff distance.

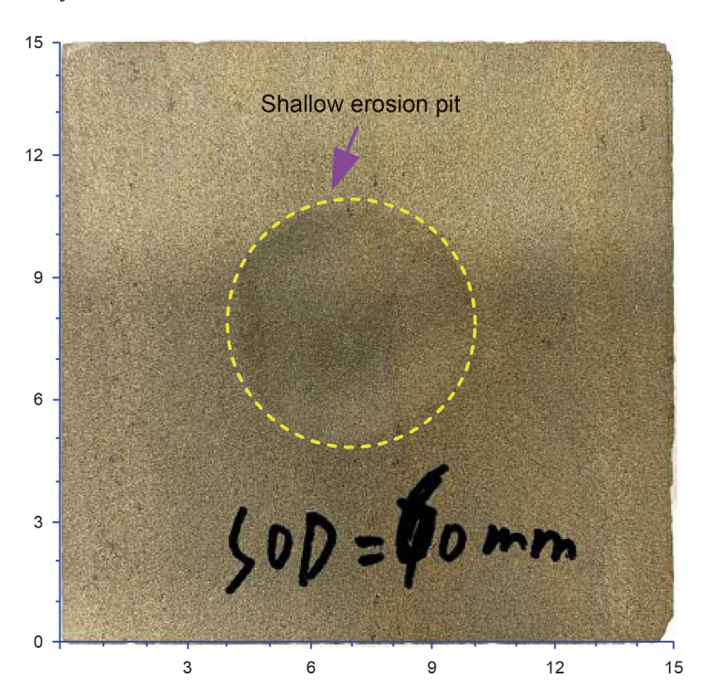


Fig. 17. Hole orphology with 60 mm standoff distance.

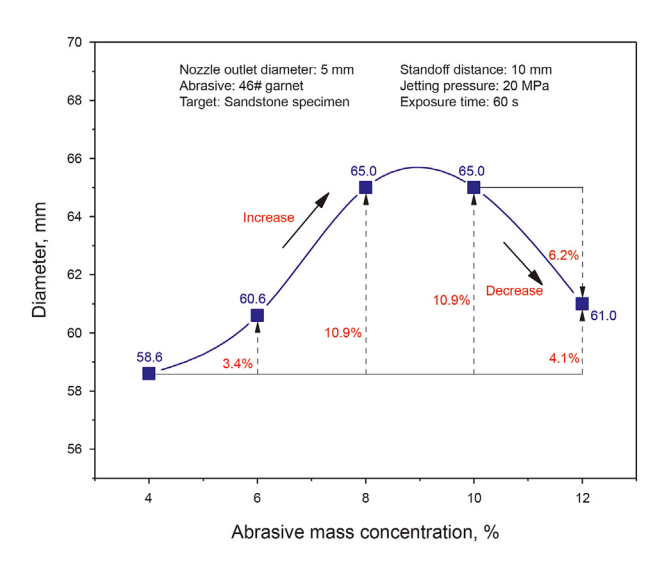


Fig. 18. Hole diameter with abrasive mass concentration.

the standoff distance increases. The volume of the hole decreases by 33.6% and 83.6% respectively as the standoff distance is raised from 0 to 30 and 60 mm.

Diffusion is one of the important characteristics of a jet and it has a close relationship with the standoff distance. As the standoff distance increases, the jet becomes more diffuse (Oh and Cho, 2014). Thus, there is a decrease in the energy density imparted to the rock free surface as the standoff distance increases. Meanwhile, the jet diffusion is beneficial for creating a large diameter hole on target rock. The SAWJ diffuses intensely because of the turbulence pulsation caused by the swirling flow (Chen et al., 2021). Therefore, the SAWJ is characterized of large impact area and short effective standoff distance. And, it's more suitable for large hole drilling such as RJD operation. The largest SAWJ-drilled hole diameter in our experiments is 72.8 mm at a standoff distance of 30 mm. Sandstone breakage morphology with 60 mm standoff distance is illustrated

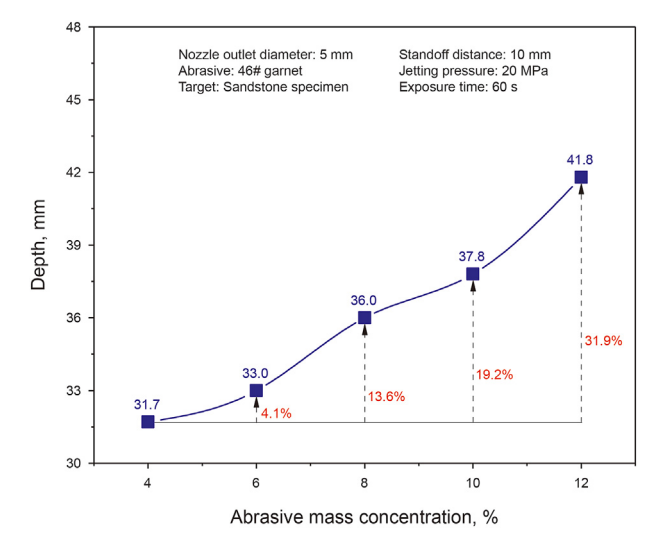


Fig. 19. Hole depth with abrasive mass concentration.

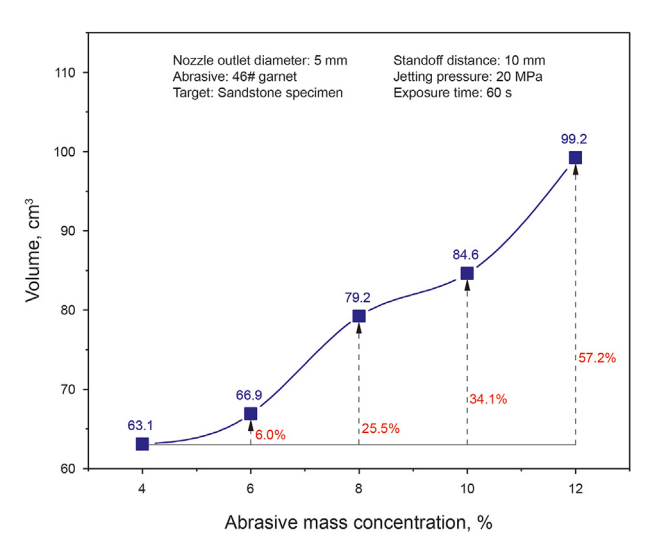


Fig. 20. Hole volume with abrasive mass concentration.

in Fig. 17. It's obviously that the impact of the SAWJ is not strong enough to create a complete hole under the condition of 60 mm standoff distance. Thus, the SAWJ's effective standoff distance under our experimental conditions is 60 mm. Besides, as analyzed above, the optimal standoff distance is 0 in an overall consideration.

3.4. Effect of abrasive mass concentration

Abrasive mass concentration is the ratio of abrasive mass to water mass in the abrasive slurry. The abrasive mass concentration has a significant impact on the rock breaking performance (Oh et al., 2019). The diameter, depth and volume of the hole with various abrasive mass concentration (4%, 6%, 8%, 10%, 12%) are illustrated in Figs. 18, 19 and 20. It can be found in Fig. 18 that the hole diameters are in 58.6–65.0 mm which is satisfied with the hole diameter requirement of RJD. The range of the hole diameters under different abrasive mass concentration is 6.4 mm, that means the degree of dispersion of the hole diameters are small. Therefore, it can be inferred that the abrasive mass concentration only has a minimal impact on the diameter of the hole. This may be explained that the diameter of the hole is influenced by the jet diffusion, but

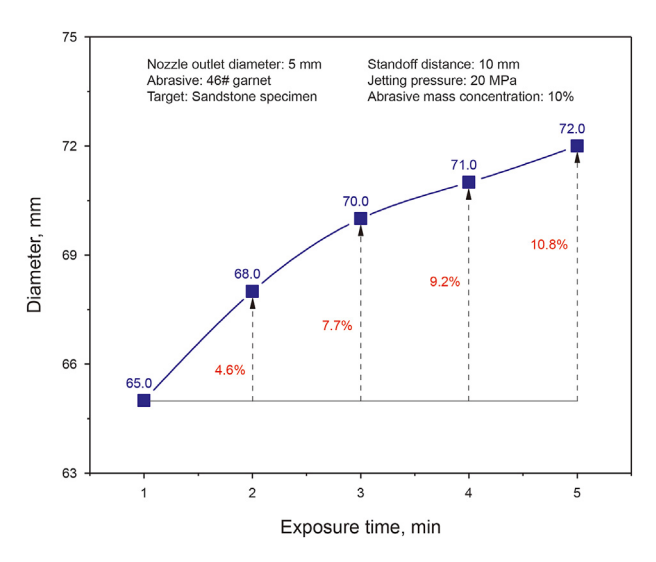


Fig. 21. Hole diameter with exposure time.

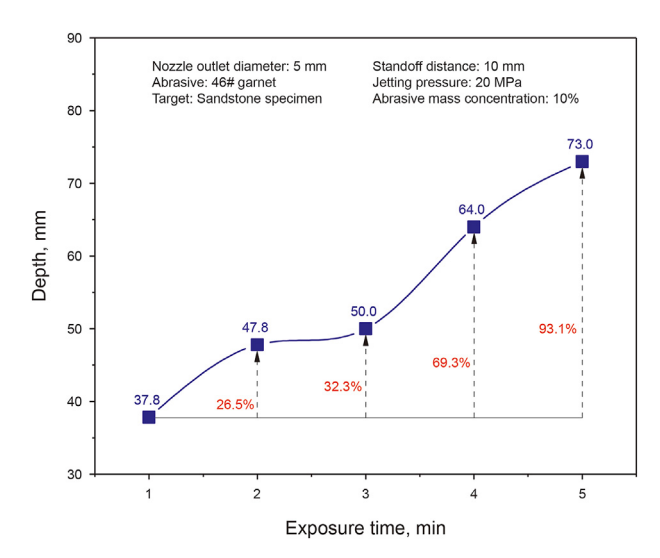


Fig. 22. Hole depth with exposure time.

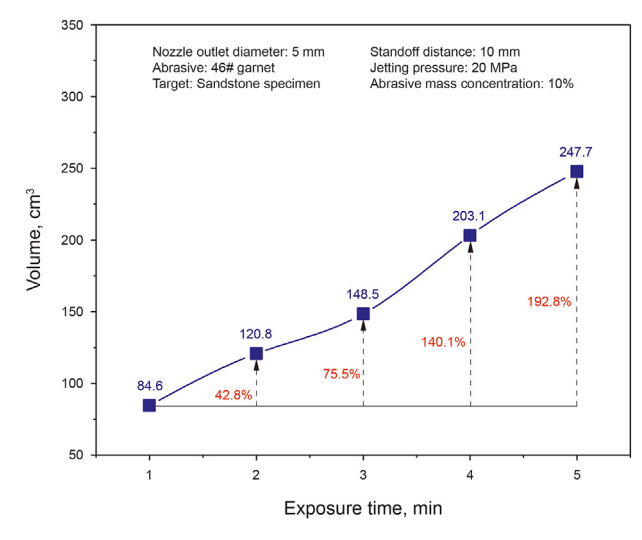


Fig. 23. Hole volume with exposure time.

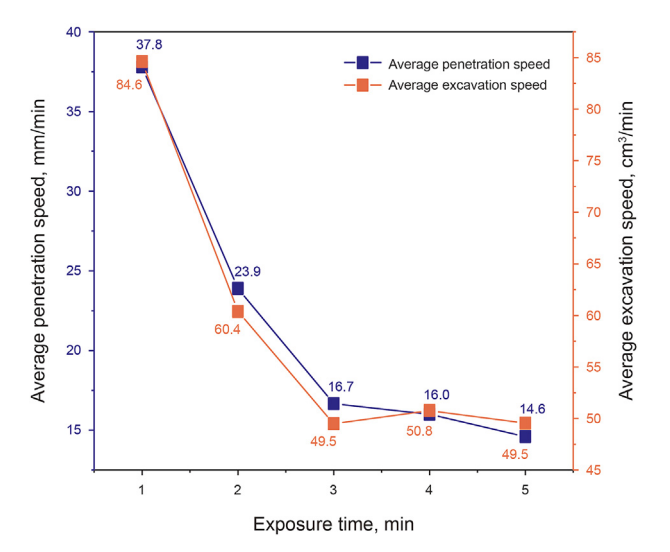


Fig. 24. Average penetration and excavation speed.

the jet diffusion is independent of the abrasive mass concentration. It can be found in Fig. 19 that the hole depth is positively associated with the abrasive mass concentration. The hole depth increases by 31.9% with the increase of abrasive mass concentration from 4% to 12%. It can be found in Fig. 20 that there is a positive correlation between the hole volume and the abrasive mass concentration. Specifically, the hole volume increases by 57.2% when the abrasive mass concentration increases from 4% to 12%.

As illustrated in Section 3.2, the higher the jet effective kinetic energy, the better the sandstone breakage performance. Besides, Eq. (3) can be rewritten as Eq. (4), because the abrasive mass is the product of the abrasive mass concentration and the water mass. As expressed in Eq. (4), it's obviously that the effective kinetic energy shows a liner correlation of the abrasive mass concentration. Thus, the higher the abrasive mass concentration, the better the SAWJ rock breaking performance. As analyzed above, the optimal abrasive mass concentration is 12% under our experimental conditions. Meanwhile, the abrasion of abrasive particle on jet nozzle and pipe assembly is not obviously neglectable (Selwin and Ramachandran, 2016). Usually, the higher the abrasive mass concentration, the more serious the nozzle and pipe assembly abrasion. Fortunately, the abrasion of abrasives on nozzle and pipe in our experiments when the abrasive mass concentration is 12% is acceptable.

$$E_{\text{effective}} = \frac{Sm_{\text{w}}PC^2}{2\rho}t = k_2S \left(k_2 = \frac{m_{\text{w}}PC^2t}{2\rho} = \text{constant}\right)$$
(4)

where S is the abrasive mass concentration, m_W is the water mass per unit time.

3.5. Effect of exposure time

Exposure time is the time that the jet impacts on the target material. The diameter, depth and volume of the hole with virous exposure time (1–5 min) are illustrated in Figs. 21, 22 and 23. It can be found in Fig. 21 that the hole diameters are in 65.0–72.0 mm. Besides, the diameter of the hole is positively correlated with the exposure time. And it increases by 10.8% as the exposure time is raised from 1 to 5 min. It can be found in Fig. 22 that the depth of the hole increases with an increase in the exposure time. The hole diameter increases by 93.1% as the exposure time is raised from 1 to 5 min. However, the average penetration speed of the SAWJ under

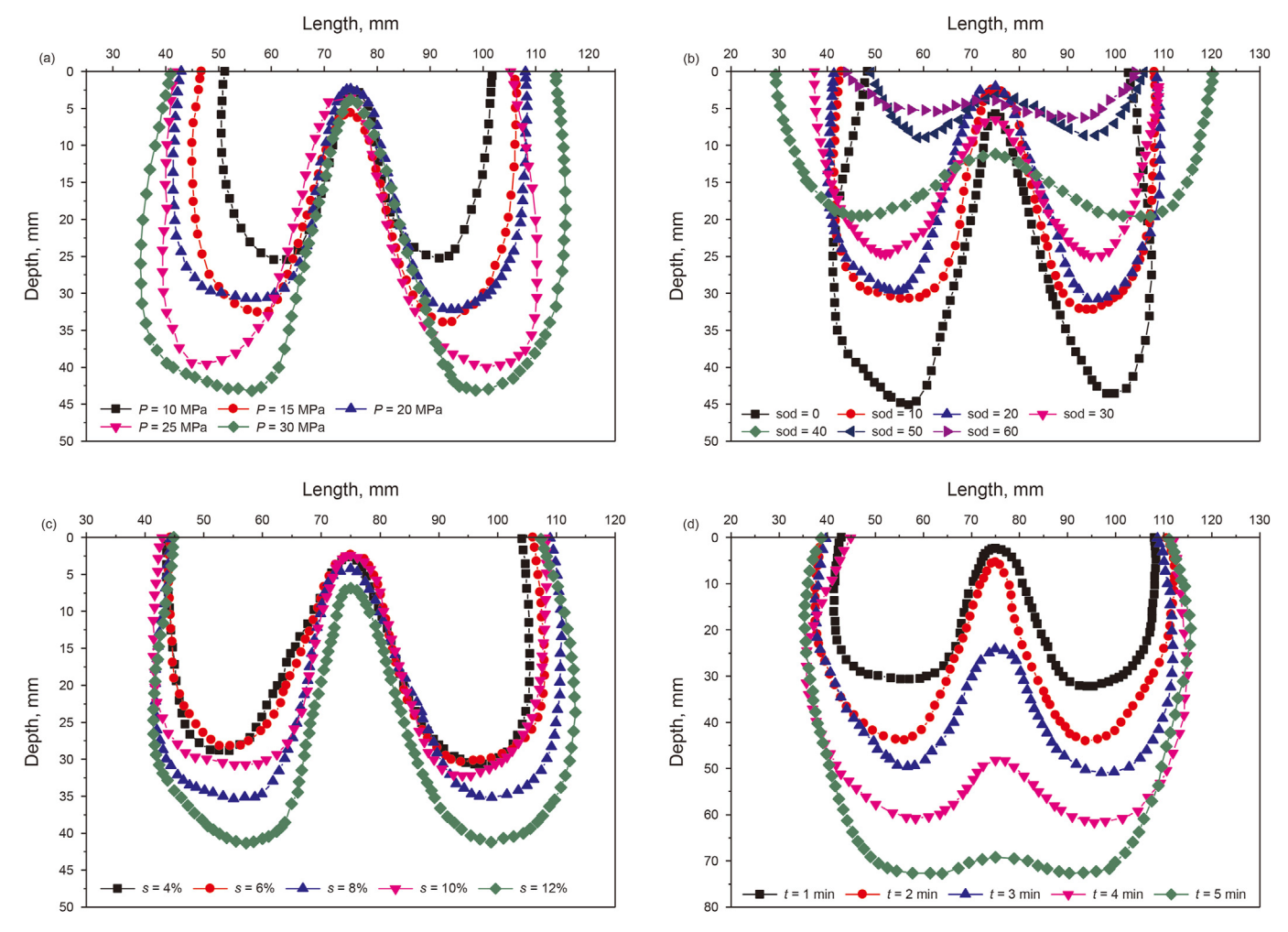


Fig. 25. SAWJ-drilled hole profiles under different parameters. (a) Jetting pressure (10–30 MPa); (b) Standoff distance (0–60 mm); (c) Abrasive mass concentration (4%–12%); (d) Exposure time (1–5 min).

different exposure time shows a decrease trend with an increase in the exposure time. The average penetration speed at the exposure time of 1 min is 2.59 times of that at the exposure time of 5 min. It can be found in Fig. 23 that the volume of the hole increases with an increase in the exposure time and it increases by 192.8% as the exposure time is raised from 1 to 5 min. But the SAWJ's average excavation speed decreases with an increase in the exposure time (Fig. 24). The average excavation speed is 49.5 cm³/min at the exposure time of 5 min, which is only 58.6 % of the average excavation speed at the exposure time of 1 min.

Impacts of abrasive particles to target rock material is the main rock removal pattern of an abrasive waterjet. Moreover, the count of abrasive particle impacts escalates linearly as the exposure time is extended. Specifically, Eq. (5) shows the effective jet kinetic energy calculation formula when only the exposure time is changed. As shown in Eq. (5), the effective kinetic energy increases with an increase in the exposure time. Thus, a longer exposure time results in a better SAWJ rock breakage performance. However, rock breaking efficiency of SAWJ (average penetration speed and average excavation speed) decreases with an increase in the exposure time (Fig. 24). This may be caused by the increased impact number between abrasive particles with exposure time. Because the collisions between abrasive particles will consume the jet energy (Oh and Cho, 2014). Since the SAWJ-drilled hole diameter with 1 min exposure time is satisfied with the requirement of RJD and

the average penetration/excavation speed decreases with exposure time, the optimal exposure time is 1 min under our experimental conditions.

$$E_{\text{effective}} = \frac{m_{\text{a}}PC^2}{2\rho}t = k_3S \left(k_3 = \frac{m_{\text{a}}PC^2}{2\rho} = \text{constant}\right)$$
 (5)

4. Discussions

4.1. Evolution of holes

Jet-drilled hole profiles are the foundation to reveal the evolution of the hole morphology. The SAWJ-drilled hole profiles are obtained by binarization method with the help of longitudinal section image of the SAWJ-drilled hole and image processing program (MATLAB). The hole profiles under different jetting pressure, different standoff distance, different abrasive mass concentration and different exposure time are shown in Fig. 25, respectively. Generally speaking, the SAWJ-drilled hole profile is "W" shaped, that indicates the high impact energy density area of a SAWJ is located in an annular region rather than the axis of the jet. Since the diameter, depth, and volume of the hole under different parameter combinations are illustrated and analyzed above, here we will



Fig. 26. SEM analysis of the surface of hole. (a) Areas of SEM analysis: A-hole edge area, B-hole wall area, C-hole bottom area, D-bulge wall area, E-bulge top area; (b) SEM analysis samples collected from the SEM observation regions; (c) SEM analysis.

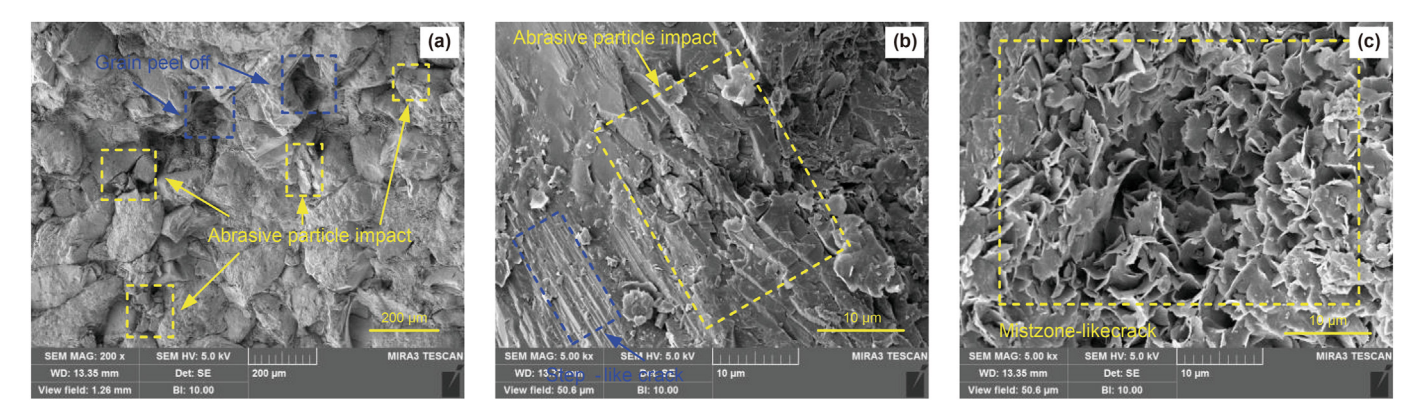


Fig. 27. Typical micromorphological characteristics of the hole. (a) The abrasive particles impact and the crystal grain is integrally peeled off; (b) The crystal grain is broken into pieces under the abrasive particles impact and the step pattern; (c) The mist zone-like pattern which is composed of quantities of flaky rock debris.

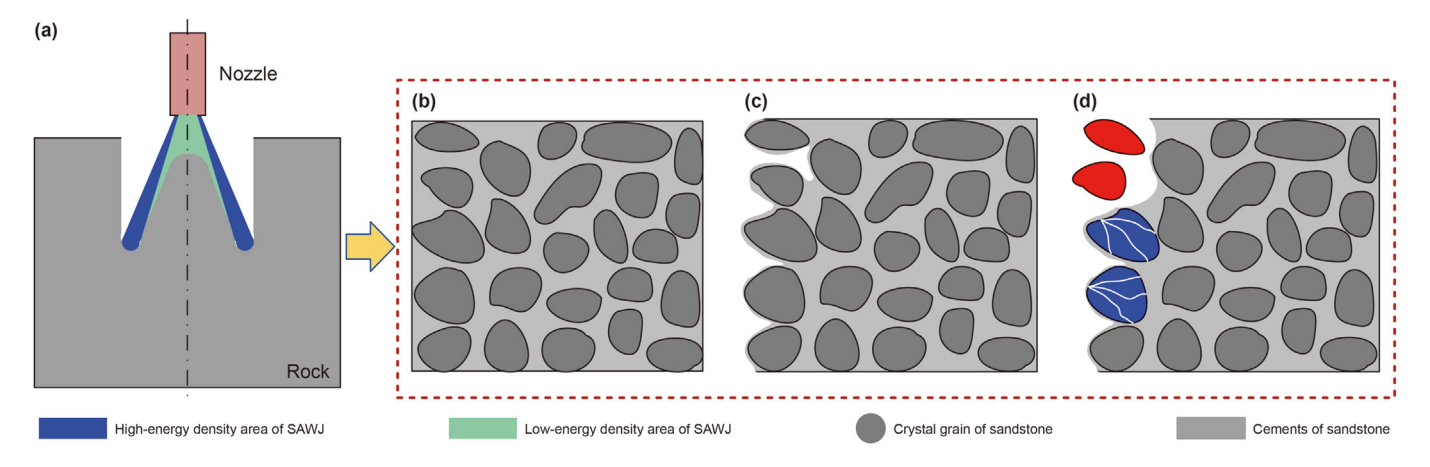


Fig. 28. Sandstone breaking process and mechanism of the SAWJ. (a) Flow filed and rock breaking characteristics of the SAWJ; (b) The composition of sandstone includes cements and crystal grain; (c) The cements are eroded during the SAWJ drilling of sandstone; (d) The integrally peeled off (red crystal grain) and broken (blue crystal grain) of the crystal grain during the SAWJ drilling of sandstone.

discuss the formation and evolution of the conical bulge.

The jet-drilled hole should permit the jet nozzle to enter it for drilling a long radial branch. However, as for SAWJ-drilled hole, the conical bulge at the hole bottom will stop the nozzle from entering the hole to some extent. In this paper, the distance between the target rock jetting surface and the peak of the conical bulge is regard as the hole depth that the nozzle can enter (h_a). As shown in Fig. 25, the jetting pressure and abrasive mass concentration only have a slight influence on the h_a . The range of h_a with different jetting pressure and different abrasive mass concentration are 3.8 and 5.0 mm, respectively (Fig. 25(a) and (c)). The range of h_a is

9.6 mm (Fig. 25(b)) under different standoff distance. Thus, it can be considered that the standoff distance has a medium influence on the h_a . With the increase in the standoff distance during SAWJ rock breaking, the radial turbulence is significantly enhanced and the diffusion angle is increased too. Furthermore, the jet impact energy density of the target rock surface will decrease as the standoff distance increases, which will change the morphology (diameter, depth, h_a) of the hole to some extent. While the exposure time has a significant impact on the h_a (Fig. 25(d)). The rang of h_a under different exposure time in our experiments is 67.5 mm, which is 17.8, 13.5 and 7.0 times of the h_a under different jetting pressure,

different abrasive mass concentration and different standoff distance respectively. What's more, the conical bulge almost disappears and the hole profile is nearly "U" shaped when the exposure time is 5 min (Fig. 25(d)). The abrasive particles will continue erode the conical bulge by the swirling flow effect of SAWJ until it disappears. And, as shown in Fig. 25(d), it can be inferred that the hole profile will transit from "W" shaped to "U" shaped with the increase of exposure time.

4.2. Rock breaking mechanism

Micro-morphology of the hole surface is used to reveal the SAWI sandstone breaking mechanism. Five typical regions are selected to do SEM (Scanning electron microscope) analysis based on the characteristics of the hole profile (Fig. 26). Five regions are the edge area, hole wall area, hole bottom area, bulge wall area and bulge top area, respectively (Fig. 26(a)). However, the results of SEM observation indicate that the micro-morphology of the mentioned five regions align with each other. Typical micro-morphology of the SAWJ-drilled hole surfaces are shown in Fig. 27. Sandstone has the characteristics of high porosity and weak crystal grain cementation. Since the mechanical strength of the cements is far less than the crystal grain, a large number of cements are eroded firstly by the SAWJ and the inter-granular cracks are formed around the crystal grain (Fig. 27(a)). Then, as depicted in the blue-dashed rectangle in Fig. 27(a), some crystal grain is integrally peeled off. Besides, as depicted in the yellow-dashed rectangle in Fig. 27(a), some crystal grain is broken by the abrasive particles impact and intra-granular fractures are formed in the crystal grain. Specially, as depicted in the yellow-dashed rectangle in Fig. 27(b), it's clear that the crystal graine is broken into pieces under the abrasive particles impact. Micromorphological characteristics of the hole surface is complex and varied. It mainly includes step pattern (Fig. 27(b)) and mist zone-like pattern (Fig. 27(c)). It is worth noting that the patterns are both tensile fractures. The mist zone-like pattern is composed of quantities of flaky rock debris (Fig. 27(c)) because of the collision of high-speed abrasive particles.

The sandstone breaking process and mechanism of the SAWJ are summarized as Fig. 28. High-energy density area of the SAWJ is in an annular region because of the swirling flow effect, which finally makes the conical bulge one of the most signification characteristics of the hole. Generally speaking, the hole profile is displayed as a "W" shape (Fig. 28(a)). Further, the hole profile will be transferred from "W"-shaped to "U"-shaped with the increase of exposure time based on our experimental results. Erosion mechanism of the SAWJ to the sandstone can be described as follows: (i) The cements of the sandstone free surface are eroded by the impact of the SAWI (from Fig. 28(b) to Fig. 28(c)) and part of the crystal grain is exposed for the lack of cements' support (Fig. 28(c)); (ii) As the cements are eroded continuously, some crystal grain which completely lose the support of cements is integrally peeled off (red crystal grain in Fig. 28(d)). And, some crystal grain is broken into pieces under the high-speed abrasive particles impact simultaneously (blue crystal grain in Fig. 28(d)); (iii) Step (i) and (ii) are happening continuously and alternately during the SAWJ drilling of sandstone. And, a hole will be created eventually under the joint action of step (i) and step (ii). Besides, the main failure mode of sandstone during SAWJ drilling is tensile failure. Given the sandstone's tensile strength is only 9.5% of its UCS, the SAWJ sandstone breakage efficiency is high.

5. Conclusions

In this paper, effect of key job parameters (jetting pressure, standoff distance, abrasive mass concentration and exposure time) on SAWJ sandstone breakage performances were experimentally studied. Diameter, depth and volume of the hole were employed to evaluate the SAWJ rock breaking performances under different parameter combinations. Then, the evolution of holes and sandstone breaking mechanism were illustrated. The following main conclusions were drawn:

- The SAWJ creates a smooth large regular hole on sandstone. The hole diameters are in 52.0–73.0 mm. Besides, there exists a conical bulge at the hole bottom. But it can be eroded by the follow-up jet and can't stop the feeding of the nozzle assembly. Thus, the SAWJ is an alternative to drill radial branches in sandstone formation.
- The SAWJ-drilled hole depth/volume increased as the jetting pressure, abrasive mass concentration and exposure time increased. Conversely, they decreased as the standoff distance increased. As for the hole diameter, it is less affected by jet parameters. The optimal parameter combination under our experimental conditions was 30 MPa, 0 mm, 12% and 1 min.
- Sandstone breaking mechanism of SAWJ are the erosion of cements, the integrally peeled off of crystal grain and the broken of crystal grain. Damage patterns of the hole surface are mainly tensile fractures, such as step pattern and mist zone-like pattern. Given the sandstone's tensile strength is only 9.5% of its UCS, the SAWJ sandstone breakage efficiency is high.
- Nozzle structure plays an important role in its rock breaking performance. Thus, in our future work, we will optimize the structure of swirling impeller nozzle. And, we will conduct some oil field test to verify the feasibility of utilizing SAWJ to drill radial branches from the perspective of industrial applications.

CRediT authorship contribution statement

Huan Li: Writing — original draft, Methodology, Investigation. **Jing-Bin Li:** Supervision, Methodology, Investigation, Funding acquisition, Conceptualization. **Chen-Rui Guo:** Writing — review & editing, Investigation. **Hao Wang:** Writing — review & editing, Investigation. **Rui Li:** Writing — review & editing, Investigation. **Zhong-Wei Huang:** Methodology, Funding acquisition.

Declaration of competing interest

The authors declare that they have no known competing financial interests or personal relationships that could have appeared to influence the work reported in this paper.

Acknowledgements

This research was funded by National Natural Science Foundation of China-CO₂ displacement and production increase mechanism in radial horizontal wells of shale oil (No. 52374018) and the Strategic Cooperation Technology Projects of CNPC and CUPB (NO. ZLZX2020-02).

References

Asgharzadeh, A., Bello, O., Grijalva, O., Freifer, R., Holzmann, J., Oppelt, J., 2017. A study of water jet techniques in radial jet drilling: establishing efficacious communication between wellbore and reservoir. Mediterr. Conf. Exhib.

Ashena, R., Mehrara, R., Ghalambor, A., 2020. Well productivity improvement using radial jet drilling. In: SPE International Conference and Exhibition on Formation Damage Control. 19–21 February (Lafayette, Louisiana, USA).

Barton, N., 1978. Suggested methods for the quantitative description of discontinuities in rock masses. Int. J. Rock Mech. Min. Sci. Geomech. Abstracts 15 (6), 319–368.

Chen, J.X., Yang, R.Y., Huang, Z.W., Li, G.S., Qin, X.Z., Li, J.B., Wu, X.G., 2021. Detached eddy simulation on the structure of swirling jet flow field. Petrol. Explor. Dev.

- 49, 929-941. https://doi.org/10.1016/S1876-3804(22)60322-7.
- Du, P., Peng, X.F., Wei, Z.D., Xu, B.X., 2022. Flow field investigation of a straight-swirling integrated jet for radial jet drilling. Energy Rep. 8, 7434–7443. https://doi.org/10.1016/j.egyr.2022.05.246.
- Fu, B.W., Zhang, S., Liu, S.H., Zhu, Z.L., 2021. Drilling performance analysis of a new type of direct-rotating mixed-jet nozzle. J. Petrol. Sci. Eng. 200, 11. https:// doi.org/10.1016/j.petrol.2020.108302.
- Gong, D.G., Qu, Z.Q., Guo, T.K., Tian, Y., Tian, K.H., 2016. Variation rules of fracture initiation pressure and fracture starting point of hydraulic fracture in radial well. J. Petrol. Sci. Eng. 140, 41–56. https://doi.org/10.1016/j.petrol.2016.01.006.
- Guo, Z.Q., Tian, S.C., Liu, Q.L., Ma, L.Y., Yong, Y.N., Yang, R.Y., 2022. Experimental investigation on the breakdown pressure and fracture propagation of radial borehole fracturing. J. Petrol. Sci. Eng. 208, 109169. https://doi.org/10.1016/ j.petrol.2021.109169.
- He, X., Chen, G.S., Wu, J.F., Liu, Y., Wu, S., Zhang, J., Zhang, X.T., 2023. Deep shale gas exploration and development in the southern Sichuan Basin: new progress and challenges. Nat. Gas. Ind. B 10, 32–43. https://doi.org/10.1016/j.ngjb.2023.01.007.
- Hong, C.Y., Yang, R.Y., Huang, Z.W., Liu, W., Chen, J.X., Cong, R.C., 2021. Experimental investigation on coal-breakage performances by abrasive nitrogen-gas jet with a conical nozzle. Int. J. Rock Mech. Min. Sci. 142, 13. https://doi.org/10.1016/ j.ijrmms.2021.104781.
- Huang, Z.W., Huang, Z., Su, Y.N., Bi, G., Li, W.C., Liu, X., Jiang, T.W., 2020. A feasible method for the trajectory measurement of radial jet drilling laterals. SPE Drill. Complet. 35, 125—135. https://doi.org/10.2118/192140-PA
- Complet. 35, 125–135. https://doi.org/10.2118/192140-PA. Huang, Z.W., Huang, Z., Su, Y.N., Li, W.C., Jiang, T.W., 2018. Where the laterals go? A feasible way for the trajectory measurement of radial jet drilling wells. In: SPE Asia Pacific Oil and Gas Conference and Exhibition. 23–25 October. Brisbane, Australia. https://doi.org/10.2118/192140-MS.
- Jia, C.Z., Zou, C.N., Li, J.Z., Li, D.H., Zheng, M., 2012. Assessment criteria,main type-s,basic features and resource prospects of the tight oil in China. Acta Pet. Sin. 33, 343–350. http://www.syxb-cps.com.cn/EN/Y2012/V33/I3/343 (in Chinese).
- Kalam, S., Afagwu, C., Al Jaberi, J., Siddig, O.M., Tariq, Z., Mahmoud, M., Abdulraheem, A., 2021. A review on non-aqueous fracturing techniques in unconventional reservoirs. J. Nat. Gas Sci. Eng. 95, 104223. https://doi.org/ 10.1016/j.jngse.2021.104223.
- Kamel, A.H., 2017. Radial jet drilling: a technical review. In: SPE Middle East Oil & Gas Show and Conference. 6–9 March. Manama, Kingdom of Bahrain. https://doi.org/10.2118/183740-MS.
- LaFollette, R.F., Izadi, G., Zhong, M., 2014. Application of multivariate statistical modeling and geographic information systems pattern-recognition analysis to production results in the eagle ford formation of south Texas. In: SPE Hydraulic Fracturing Technology Conference. 4—6 February, The Woodlands, Texas, USA. https://doi.org/10.2118/168628-MS.
- Li, G.S., Tian, S.C., Zhang, Y.Q., 2020. Research progress on key technologies of natural gas hydrate exploitation by cavitation jet drilling of radial wells. Petroleum Science Bulletin 5 (3), 349–365. https://doi.org/10.3969/j.issn.2096-1693.2020.03.030 (in Chinese).
- Li, H., Huang, Z.W., Li, J.B., Cheng, K., Jiang, T.W., Xiong, C., 2023. Performances of different abrasive materials during swirling impeller abrasive water jet drilling of granite. Rock Mech. Rock Eng. 56 (6), 4343–4361. https://doi.org/10.1007/ s00603-023-03222-5
- Li, H., Huang, Z.W., Li, J.B., Li, X.J., Jiang, T.W., Chen, J.X., 2022. Rock breaking characteristics by swirling impeller abrasive water jet (SAWJ) on granite. Int. J. Rock Mech. Min. Sci. 159, 105230. https://doi.org/10.1016/j.ijrmms.2022.105230.
- Li, J.B., Dai, J.C., Huang, Z.W., Zhang, G.Q., Liu, X., Li, H., 2021. Rock breaking characteristics of the self-rotating multi-orifice nozzle for sandstone radial jet rrilling. Rock Mech. Rock Eng. 54, 5603–5615. https://doi.org/10.1007/s00603-021-02567-2
- Li, J.B., Li, G.S., Huang, Z.W., Song, X.Z., Yang, R.Y., Peng, K.W., 2015. The self-propelled force model of a multi-orifice nozzle for radial jet drilling. J. Nat. Gas Sci. Eng. 24, 441–448. https://doi.org/10.1016/j.jngse.2015.04.009.
- Ma, G.R., Li, J.B., Li, H., Zhang, J., Chang, W.J., 2021. Study on pore forming characteristics of carbonate rock broken by swirling abrasive water jet. Fluid Mach. 49 (11), 12–17. https://doi.org/10.3969/j.issn.1005-0329.2021.11.003 (in Chinese).
- Ma, Y.Z., Moore, W.R., Gomez, E., Clark, W.J., Zhang, Y., 2016. Tight gas sandstone

- reservoirs, Part 1: overview and lithofacies. Unconv. Oil Gas Resour. 405–427. https://doi.org/10.1016/B978-0-12-802238-2.00014-6.
- Mojid, M.R., Negash, B.M., Abdulelah, H., Jufar, S.R., Adewumi, B.K., 2021. A state-of-art review on waterless gas shale fracturing technologies. J. Petrol. Sci. Eng. 196, 108048. https://doi.org/10.1016/j.petrol.2020.108048.
- Nagar, A., Savelyev, A., Mukerjee, A., Hatchell, I., Jelsma, H., Maniar, C., Bhad, N., Pathak, S., Shrivastava, P., Nekkanti, S., Bohra, A., Vermani, S., 2020. Radial jet drilling improves injectivity & conformance in high permeability layered sandstone reservoir across mangala, bhagyam & aishwarya onshore fields in India. In: SPE Asia Pacific Oil & Gas Conference and Exhibition. 17–19 November. Virtual. https://doi.org/10.2118/202221-MS.
- Oh, T.M., Cho, G.C., 2014. Characterization of effective parameters in abrasive waterjet rock cutting. Rock Mech. Rock Eng. 47, 745–756. https://link.springer. com/article/10.1007/s00603-013-0434-3.
- Oh, T.M., Cho, G.C., 2016. Rock cutting depth model based on kinetic energy of abrasive waterjet. Rock Mech. Rock Eng. 49, 1059–1072. https://link.springer. com/article/10.1007/s00603-015-0778-y.
- Oh, T.M., Joo, G.W., Cho, G.C., 2019. Effect of abrasive feed rate on rock cutting performance of abrasive waterjet. Rock Mech. Rock Eng. 52, 3431–3442. https://link.springer.com/article/10.1007/s00603-019-01784-x.
- Pankaj, P., Shukla, P., Yuan, G., Zhang, X., 2018. Evaluating the impact of lateral landing, wellbore trajectory and hydraulic fractures to determine unconventional reservoir productivity. In: SPE Europec Featured at 80th EAGE Conference and Exhibition. 11–14 June. Copenhagen, Denmark. https://doi.org/10.2118/ 190860-MS
- Salimzadeh, S., Grandahl, M., Medetbekova, M., Nick, H.M., 2019. A novel radial jet drilling stimulation technique for enhancing heat recovery from fractured geothermal reservoirs. Renew. Energy 139, 395–409. https://doi.org/10.1016/ i.renene.2019.02.073.
- Salimzadeh, S., Zhang, X., Kear, J., Chen, Z., 2020. Directional hydraulic fracturing using radial jet drilling technology. Rock Mech. GeoMech. Symp.
- Selwin, K., Ramachandran, S., 2016. Optimization of profile and material of abrasive water jet nozzle. In: 2nd International Conference on Frontiers in Automobile and Mechanical Engineering. Iop Publishing Ltd, Sathyabama Univ, Chennai, India
- Wang, B., Li, G.S., Huang, Z.W., Li, J.B., Zheng, D.B., Li, H., 2016. Hydraulics calculations and field application of radial jet drilling. SPE Drill. Complet. 31 (1), 71–81. https://doi.org/10.2118/179729-PA.
- Wang, T.Y., Guo, Z.Q., Li, G.S., Ma, Z.C., Yong, Y.N., Chang, X., Tian, S.C., 2023. Numerical simulation of three-dimensional fracturing fracture propagation in radial wells. Petrol. Explor. Dev. 50 (3), 699–711. https://doi.org/10.1016/S1876-3804(23)60421-5.
- Wen, H.T., Yang, R.Y., Lu, M.Q., Huang, Z.W., Hong, C.Y., Cong, R.C., Qin, X.Z., 2023. Experimental comparisons of different cryogenic fracturing methods on coals. J. Petrol. Sci. Eng. 220, 111250. https://doi.org/10.1016/j.petrol.2022.111250.
- Xiong, C., Huang, Z.W., Shi, H.Z., Shi, X.X., Zhang, B., Chalaturnyk, R., 2022. Experimental investigation into mixed tool cutting of granite with stinger PDC cutters and conventional PDC cutters. Rock Mech. Rock Eng. 55, 813–835. https://link.springer.com/article/10.1007/s00603-021-02680-z.
- Xu, Y., Lun, Z.M., Pan, Z.J., Wang, H.T., Zhou, X., Zhao, C.P., Zhang, D.F., 2022. Occurrence space and state of shale oil: a review. J. Petrol. Sci. Eng. 211, 110183. https://doi.org/10.1016/j.petrol.2022.110183.
- Yang, R.Y., Hong, C.Y., Huang, Z.W., Song, X.Z., Zhang, S.K., Wen, H.T., 2019. Coal breakage using abrasive liquid nitrogen jet and its implications for coalbed methane recovery. Appl. Energy 253, 113485. https://doi.org/10.1016/ j.apenergy.2019.113485.
- Yang, R.Y., Huang, Z.W., Li, G.S., Chen, J.X., Wen, H.T., Qin, X.Z., 2022. Investigation of hydraulic jet multistage cavity completion in coalbed methane horizontal wells. J. China Coal Soc. 47, 3284–3297 (in Chinese).
- Yang, R.Y., Wen, H.T., Huang, Z.W., Zhang, B., Wang, H.Z., Wang, B., Dubinya, N., 2023. Experimental investigation on fracture characteristics by liquid nitrogen compound fracturing in coal. Fuel 340, 127434. https://doi.org/10.1016/ j.fuel.2023.127434.
- Zhou, M.M., Li, H., Li, G.S., Huang, Z.W., Li, J.B., Cheng, K., Hu, J.R., 2023. Study on applicability of swirling abrasive water jet drilling in reservoirs. Fluid Mach. 51, 1–7. https://doi.org/10.3969/j.issn.1005-0329.2023.01.001 (in Chinese).